THE JOURNAL OF PHYSICAL CHEMISTRY B

Article

pubs.acs.org/JPCB

Temperature-Dependent Dynamic Response to Flash Heating of Molecular Monolayers on Metal Surfaces: Vibrational Energy Exchange

Christopher M. Berg, Yuxiao Sun, and Dana D. Dlott*

School of Chemical Sciences, University of Illinois at Urbana−Champaign, Box 01-6 CLSL, 600 South Mathews Avenue, Urbana, Illinois 61801, United States

ABSTRACT: An ultrafast nonlinear coherent laser spectroscopy termed vibrational sum-frequency generation (SFG) was used to monitor vibrational transitions of a self-assembled monolayer (SAM) of 4-nitrobenzenethiolate (NBT) on Au after Au flash heating. Ultrafast thermoreflectance measurements showed the surface temperature jumps ΔT were in the 35−250 K range. The NBT symmetric and antisymmetric nitro stretches $\nu_s NO_2$ and $\nu_{as} NO_2$ and a phenyl ring stretch νCC were probed. Flash heating caused these transitions to lose intensity, shift, and broaden. The time dependences all had overshoot−decay−plateau structures. In the long-lived plateau, the SAM was in thermal equilibrium with the hot Au surface. The SFG plateau intensity losses of $\nu_s NO_2$ and νCC, two vibrations with parallel transition moments, were identical, indicating that the SFG intensity loss was caused by thermally induced SAM orientational disorder. The T-jump-induced frequency shifts of $\nu_s NO_2$ and $\nu_{as} NO_2$ were identical and opposite in sign. The rise times of the shifts were identical and equal to the ∼3.5 ps time constant for the rise of Au surface temperature, which indicates that both shifts were caused by anharmonic coupling to the same lower-energy vibration. The temperature dependence of the $\nu_s NO_2$ shift and width indicated that this vibration was the ∼480 cm^{-1} nitro bend. The $\nu_s NO_2$ temperature dependence was interpreted using a vibrational energy exchange mechanism between the nitro stretch and bend.

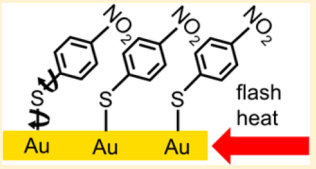

1. INTRODUCTION

In this study, we examine the time-dependent vibrational response of molecular adsorbates on flash-heated Au surfaces and how the response depends on which molecular vibration was probed and the size of the temperature jump (T-jump) ΔT, where ΔT ranged from 35 to 250 K. In several previous studies, our group had developed techniques to controllably flash-heat Au surfaces with self-assembled monolayer (SAM) adsorbates, where the specific vibrational transitions could be probed by ultrafast vibrational spectroscopy.[1−6] The specific type of spectroscopy used is termed broad-band multiplex vibrational sum-frequency generation with nonresonant suppression (SFG),[5,7] and this method provided high-quality time-resolved vibrational spectra of monolayers, despite the short time intervals (picoseconds) and the small number of molecules (∼10^{11}) being probed.[2] The specific SAM studied here was 4-nitrobenzenethiolate (NBT), and we used SFG to probe both nitro and phenyl groups. The experimental concept, where the Au surface was flash-heated while SFG probed the SAM[2] is depicted in Figure 1a.

The vibrational dynamics of molecules adsorbed on metal surfaces play an important role in many chemical and physical processes, such as heterogeneous catalysis[8,9] and molecular electronics.[10] Our previous studies[1,2,4−6] revealed features that were relevant to those processes. Because the T-jumps persist for just 10 μs[4] with flash heating, we can superheat molecular adsorbates well above the usual decomposition temperature without substantial decomposition because the molecules do not have enough time to decompose.[2] In this way, we can pump a great deal of vibrational energy into the adsorbates. This energy will flow from the hot metal surface, through the Au−S surface linker groups (Figure 1a), into the rest of the molecule.[2] Flash-heating and flash-superheating studies allow us to investigate highly vibrationally excited adsorbed species on surfaces and their interactions with laser-generated hot surface electrons and phonons.[6] In addition, we can probe vibrational energy transport by monitoring vibrational reporting groups on specific parts of the absorbates.[3] In this way, we have measured the flow of heat in several types of molecular wires consisting of long-chain alkanes[1,2] or linear polyphenyls.[6] In the alkanes,[2,4] for instance, where SFG was used to probe the terminal methyl groups, energy flowed from the hot Au surface, through the linker groups, and along the length of the alkane chains. The energy transport was ballistic with a speed of 0.95 km s^{-1}.[2,4]

In a recent study,[1] we showed how we used time-resolved broad-band optical reflectivity to monitor Au surfaces flash-heated by blue (400 nm) femtosecond pulses. These flash-heating pulses could produce T-jumps where ΔT was up to 500 K.[1] At shorter delay times, the Au transient reflectivity was dominated by optically excited hot electrons.[11] The hot Au electrons decayed by exciting Au phonons in a few picoseconds. After the electrons and phonons equilibrated, the Au surface remained at a well-defined high temperature for a time, estimated on the basis of thermal conduction to be ∼10 μs.[4]

Special Issue: James L. Skinner Festschrift

Received: October 30, 2013
Revised: November 27, 2013

   dx.doi.org/10.1021/jp410728j | J. Phys. Chem. B XXXX, XXX, XXX−XXX

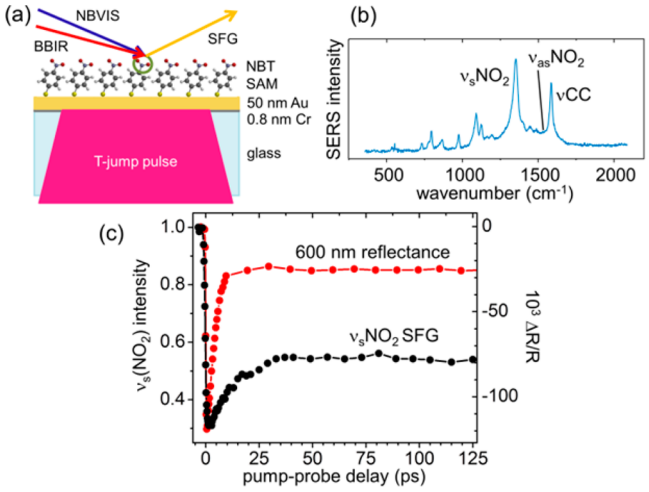

Figure 1. (a) Schematic of flash-heating experiments. A self-assembled NBT monolayer (SAM) was adsorbed on Au. After Au was flash-heated, SFG was used to probe nitro stretching or ring stretching transitions of NBT. The SFG probe used simultaneous broad-band IR (BBIR) and narrow-band visible (NBVIS) pulses. (b) Surface-enhanced Raman spectrum of a NBT monolayer showing the three transitions probed by SFG. (c) An example of a Au surface reflectance transient and its associated NBT $\nu_s NO_2$ SFG transient. The reflectance change in the plateau region gives the magnitude of the T-jump, ΔT = 190K.

We have calibrated the transient reflectivity so that we can optically determine the surface temperature. We can produce and measure T-jumps up to 500 K on Au, but because SFG experiments require signal averaging over many thousands of laser shots, the practical maximum for SFG spectroscopy was $\Delta T \approx 250$ K, limited by multipulse optical damage of the Au layer.[1]

A flash-heating vibrational transient, defined as the time-dependent SFG signal intensity change of a flash-heated adsorbate, can exhibit several features. Usually, the SFG intensity decreases upon flash heating.[2] During the first few picoseconds, the effects of hot Au surface electrons may be observed.[6] The hot electrons can generate vibrational excitations on adsorbates. The Franck−Condon principle predicts that electrons, being of low mass, will preferentially excite higher-frequency vibrations. Electron-excited vibrations can be directly observed by SFG in several ways.[1] The most significant way is when the hot electrons excite the vibration being probed. Such an excitation depletes the ground state, reducing the SFG intensity. After the surface has a well-defined temperature and the SAMs are in equilibrium with the surface, the SFG transients will have a plateau that persists long after the end (~200 ps) of our delay scans. The SFG intensity loss in the plateau region has been attributed to thermally induced disordering of the SAM.[2,4,12] The plateau has been shown to not result from SAM thermal decomposition or SAM decomposition because we observed the SFG signals returning to their original values after the T-jump decayed.[1]

We have also shown that the vibrational spectra that we obtained were of sufficiently high quality that we could measure the time dependence of the vibrational frequency shifts and spectral widths of the more intense transitions.[1] Our ability to simultaneously measure temperature-dependent shifts and widths allows us investigate the fundamental mechanisms of vibrational dephasing of adsorbates. In the 1970s, an insightful model for these processes, based on vibrational energy exchange, was developed by Harris and co-workers and was applied to crystalline durene (1,2,4,5-tetramethylbenzene).[13−15] In subsequent works by other groups, it was applied to naphthalene crystals[16,17] and to a variety of molecular adsorbates.[8,9] This vibrational energy exchange model attributes temperature-dependent frequency shifts $\Delta\omega$ and widths [expressed in units of effective inverse line width $\Delta(\pi c T_2^{\text{eff}})^{-1}$] of a higher-frequency probed vibration Q with frequency ν_Q to energy exchange with a specific lower-energy mode q with frequency ν_q. Here "higher-frequency" means $h\nu_Q/kT \ll 1$, and "lower-frequency" means $h\nu_q/kT \approx 1$; therefore, the thermal population of the probed mode is always small, but the population of the lower-frequency mode increases significantly as temperature is increased. The magnitudes of $\Delta\omega$ and $\Delta(\pi c T_2^{\text{eff}})^{-1}$ were determined by the quartic anharmonic coupling $\langle V_{QQqq}^{(4)} \rangle$ between the lower-energy mode and the higher-energy probed mode and the lifetime τ of the lower-energy mode. The model is valid in the intermediate exchange limit where $\Delta\omega\tau \approx 1$. The model is easiest to use when the higher-energy vibration couples to a single lower-energy mode, although extending it to multiple lower-energy modes[16] is possible. In the case of a single mode, the model predicted that Arrhenius plots of $\Delta\omega$ and $\Delta(\pi c T_2^{\text{eff}})^{-1}$ (plots of the log of these quantities versus $1/T$) would be linear, and the slopes would be identical and equal to the energy $E_a = h\nu_q$ of the lower-energy mode fundamental. The $\Delta\omega$ and the $\Delta(\pi c T_2^{\text{eff}})^{-1}$ y-axis intercepts together give the values of the anharmonic coupling $\langle V_{QQqq}^{(4)} \rangle$ and the lower-energy state lifetime τ. The model would be demonstrably invalid if the values of E_a, $\langle V_{QQqq}^{(4)} \rangle$, and τ were unreasonable. Reasonable values of these parameters would consist of an E_a that corresponded to a lower-energy vibration expected to couple well to the probed vibration, $\langle V_{QQqq}^{(4)} \rangle$ in the range of a few cm^{-1} to a few tens of cm^{-1}, and τ of a few picoseconds.[14]

In the rest of this paper, we will describe the experimental techniques and present measurements on three NBT vibrational transitions, $\nu_s NO_2$, $\nu_{as} NO_2$, and νCC. The nitro stretching transitions are predominantly localized on the nitro group.[18] The νCC phenyl ring stretch in nitrobenzenes is best described as symmetric stretching along the molecular long axis.[18,19] The surface-enhanced Raman spectrum of NBT adsorbates[20] in Figure 1b shows the approximate frequencies of these transitions. (This spectrum was obtained on Ag rather than Au, which is expected to have only a minor effect on these transitions.) Then, we will discuss how our experiments reveal the intricacies of adsorbate flash heating, as observed in SFG T-jump transients, and we will apply the vibrational energy exchange model to the $\nu_s NO_2$ transition.

2. EXPERIMENTAL SECTION

The experimental technique was described previously,[1] where we demonstrated that we could measure the response of the symmetric nitro stretch transition $\nu_s NO_2$ of NBT (1344 cm^{-1}) with ΔT = 35 and 175 K. The $\nu_s NO_2$ SFG transition was intense enough that we have been able to measure its response as a function of ΔT over the range ΔT = 35−250 K. The $\nu_{as} NO_2$ (~1540 cm^{-1}) and νCC (1565 cm^{-1}) transitions were significantly weaker, and we can study their response only with larger ΔT = 190 K.

Each sample consisted of a 50 × 50 mm^2 glass substrate with a thin (0.8 nm) Cr adhesion layer[2,4] and a 50 nm Au layer. The metallized substrates were soaked in 1 mM ethanol solutions of

dx.doi.org/10.1021/jp410728j | J. Phys. Chem. B XXXX, XXX, XXX−XXX

NBT for 24 h to produce well-ordered SAMs. As depicted in Figure 1a, the *T*-jump pulses were incident on the back side (the substrate side) of the metal film, while the NBVIS and BBIR probe pulses were incident on the front side (the side with the SAM) at a 60° angle. The beam diameters were engineered so that the probed region had a *T*-jump that was nearly spatially uniform. The *T*-jump, NBVIS, and BBIR pulses had nominally Gaussian profiles with beam diameters ($1/e^2$ points) of 700, 350, and 125 μm, respectively. The effective size of the probed region was determined by the smaller of the two overlapping probe beam profiles, which was the elliptical 125 × 250 μm^2 footprint of the BBIR beam,[1] and this probed region was much smaller than the 700 μm diameter flash-heated spot.

The *T*-jump pulses were 400 nm and ~200 fs in duration, with up to 70 μJ of energy. The NBVIS pulses, created by passing 800 nm femtosecond pulses through a Fabry–Perot étalon, were picosecond pulses with 7 μJ energies, spectral widths of 10 cm^{-1}, and time-asymmetric profiles.[7,21] The BBIR pulses (fwhm = 200 cm^{-1}) were tuned to either 7.4 μm to study $\nu_s NO_2$ or 6.5 μm to study $\nu_{as} NO_2$ and νCC. The BBIR pulse duration was 250 fs, and pulse energies were ~10 μJ. A temporal delay of ~300 fs was used between BBIR and NBVIS pulses to suppress Au nonresonant signals.[7] The samples were mounted on a motorized *xy* positioner that translated the sample through the laser beams using a Lissajous pattern.[1] As discussed previously, we have shown that we can arrange conditions so that there is negligible laser damage of the Au coating or the NBT SAM during the multimillion laser shots needed to acquire data.[1]

We used Au reflectance at 600 nm to monitor the Au surface temperature. After the flash-heated surface comes to thermal equilibrium, the fractional reflectance change at 600 nm, in the longer-time plateau region of the transient (Figure 1c), is related to ΔT by[1,22]

$$\frac{\Delta R}{R}(600\ \text{nm}) = -1.32(\pm 0.02) \times 10^{-4} \Delta T \quad (1)$$

We have previously shown[1] that adsorbing a SAM on Au did not measurably affect the Au surface reflectance transients. Because the maximum surface reflectance change was <1%, the reflection transients had negligible effect on the SFG signal intensities, except possibly at the few percent level near $t = 0$.

The relationship between ΔT and the 400 nm flash-heating beam fluence varied a bit from sample to sample, presumably due to small variations in Cr layer thickness and absorbance. We made a batch of 13 identical substrates, and then, we determined a fluence vs. ΔT calibration curve using two of the substrates. The rest of the substrates were then coated with a SAM and used for SFG measurements.

3. RESULTS

Figure 1c shows a typical 600 nm reflectance flash-heating transient and the corresponding NBT SAM SFG intensity transient for $\nu_s NO_2$. Flash heating caused the reflectance and the SFG intensities to decrease. Both types of transients have the structures that we call "overshoot-decay-plateau".[1,6] On the basis of the 600 nm reflectance plateau, ΔT = 190 (±5) K in Figure 1c. The reflectance overshoot, which onsets instantaneously, was caused by the creation of nonequilibrium Au hot electrons, the plateau represented the equilibrium Au reflectivity at the higher temperature, and the 3.45 (±0.09) ps decay represented the electron–phonon equilibration process. The SFG intensity transient in Figure 1c is the fractional change in the integrated area of the $\nu_s NO_2$ transition. The SFG overshoot is attributed to effects of hot electrons, based on its instantaneous onset.[1,6] The mechanism involves hot electrons exciting the probed $\nu_s NO_2$ modes, causing SFG intensity loss due to ground-state depletion.[1] The decay to the plateau represents the vibrational lifetime T_1 of $\nu_s NO_2$ (convolved with the decay of the hot electrons), and the decay mechanism is presumably intramolecular energy transfer from $\nu_s NO_2$ to other nitro and phenyl modes.[18] The SFG plateau represents a SAM in thermal equilibrium with a hot Au surface. The plateau intensity loss is attributed to thermal disorder of the SAM layer, caused at least in part by rotations around the Au–S or S–phenyl bonds (see the inset in Figure 6a). It is interesting that the temperature of the Au surface (215 °C) is clearly above the thermal decomposition temperature of the SAM layer (~140 °C);[23] therefore, the NBT SAM is superheated and kinetically unstable with respect to thermal decomposition. No detectable decomposition, which would result in permanent SFG signal loss, was observed in these measurements. The total time that each location on the sample was subjected to elevated temperature was milliseconds. Apparently, the total time spent at high temperature was not long enough to significantly decompose the SAM.

Figure 2 shows some representative time-dependent SFG spectra of $\nu_s NO_2$ (Figure 2a) and $\nu_{as} NO_2$ and νCC (Figure 2b),

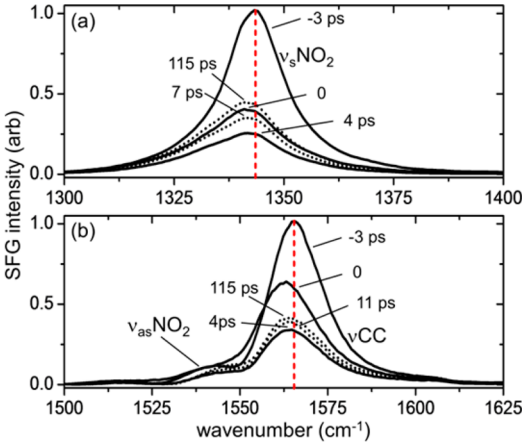

Figure 2. (a) SFG spectra of $\nu_s(NO_2)$ at indicated delay times after a pulse that flash-heated the Au surface an amount ΔT = 190 K. (b) SFG spectra under the same flash-heating conditions, in a region that contains several transitions. The two larger ones, $\nu_{as} NO_2$ and νCC, were analyzed.

where ΔT = 190 K. The $\nu_s NO_2$ transition was well-separated from the others; therefore, it was analyzed using the method of moments, where $M^{(i)}$ represents the *i*th moment. We computed the integrated intensity $M^{(0)}$, frequency shift $M^{(1)}$, and width $[M^{(2)}]^{1/2}$. The method of moments does not rely on preconceptions about the line shape function. The $\nu_{as} NO_2$ and νCC transitions were in a congested region with overlapping transitions; therefore, the areas, shifts, and widths were instead determined by a method that was less accurate than the method of moments. We fit each spectrum to the sum of four Voigt line shape functions, as illustrated in Figure 3. The use of Voigt functions was intended as a fitting artifice only and should not imply any a priori assumptions about the actual line shapes, the mechanisms responsible for the line width, or the number of transitions in this region. Four Voigt functions

dx.doi.org/10.1021/jp410728j | J. Phys. Chem. B XXXX, XXX, XXX–XXX

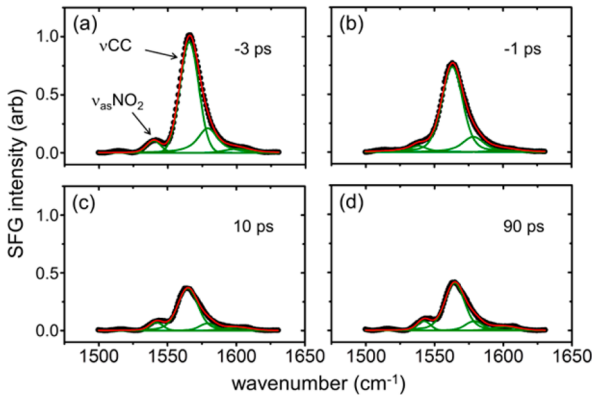

Figure 3. Examples of the fitting procedure used to determine the intensities and shifts of the $\nu_{as}NO_2$ and νCC transitions. The flash-heating pulses created a Au T-jump of ΔT = 190 K. Black circles are experimental data. Four Voigt functions (green) were used to fit each spectrum, and the red curves are the sum of those functions. Only the two Voigt functions needed to fit $\nu_{as}NO_2$ and νCC were used in the data analysis.

represented the minimum needed to accurately fit the spectrum, but only the Voigt functions used to fit $\nu_{as}NO_2$ and νCC were used in the data analysis. Due to the quality of the data, we were able to analyze only results obtained at ΔT = 190 K. Using the Voigt fitting method, we frequently found that the shift data was more reliable than the intensity data. The intensity measurements were susceptible to small laser intensity variations and small shifts in the baseline, whereas the shifts were insensitive to those factors. We were able to extract reliable intensity data for νCC, reliable shift data for νCC and $\nu_{as}NO_2$, and reliable width data for neither.

Figures 4 and 5 show the time-dependent areas (Figure 4), shifts (Figure 5a), and widths (Figure 5b) for the ν_sNO_2

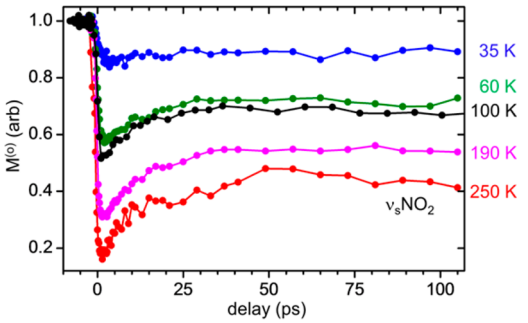

Figure 4. Time dependence of the ν_sNO_2 SFG intensity after flash heating to the indicated values of ΔT. The intensities were determined by computing the zeroth moments $M^{(0)}$ of the spectra, equivalent to the wavelength-integrated intensities.

transition at several values of ΔT. We are not sure how to interpret the small 1−2 ps spike sometimes seen in the shift and width data near t = 0,[1] but it is most likely an artifact involving the hot electron population, possibly a modulation of the SFG signal at shorter delays by the ∼1% change in Au reflectivity. In any case, in this study, we are primarily concerned with the plateau values of the shift and width. Figure 6a compares SFG intensity transients at ΔT = 190 K for νCC and ν_sNO_2. The overshoot of νCC was minimal. It is significant that the fractional SFG intensity losses in the plateau regions were identical for both transitions.

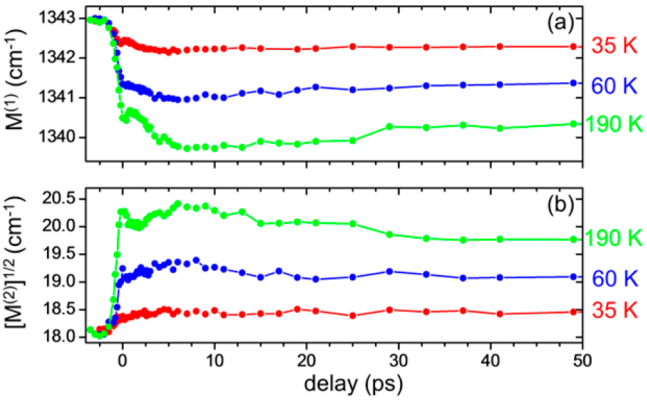

Figure 5. (a) Peak shifts and (b) peak widths of the ν_sNO_2 SFG transition, after flash heating to the indicated values of ΔT. Shifts and widths were determined by computing the first and second moments $M^{(1)}$ and $M^{(2)}$ of the SFG spectra.

Figure 6b compares the peak shift transients at ΔT = 190 K of ν_sNO_2, $\nu_{as}NO_2$, and νCC. All three transients have rapidly rising red shifts in the first few picoseconds, with maximum red shift values of 2.5, 2.5, and 0.4 cm^{-1} for ν_sNO_2, νCC, and $\nu_{as}NO_2$, respectively. In the plateau regions, νCC had a red shift of 1.0 cm^{-1}, ν_sNO_2 had a red shift of 3.0 cm^{-1}, and $\nu_{as}NO_2$ had a blue shift of 3.0 cm^{-1}. The most striking feature of Figure 6b is how, for ν_sNO_2 and $\nu_{as}NO_2$, the plateau shifts were equal and opposite, and the rates of growth of these shifts were essentially identical. These observations are strongly suggestive that the equal and opposite shifts of this pair of symmetric and antisymmetric nitro stretch modes have a common origin.

Following protocols established by Harris and co-workers,[14] for the ν_sNO_2 transition, we made an Arrhenius plot of the shift and width in Figure 7. The plotted values were the average over the plateau regions, and the error bars represent one standard deviation of this average. The shift $\Delta\omega$ was the first moment

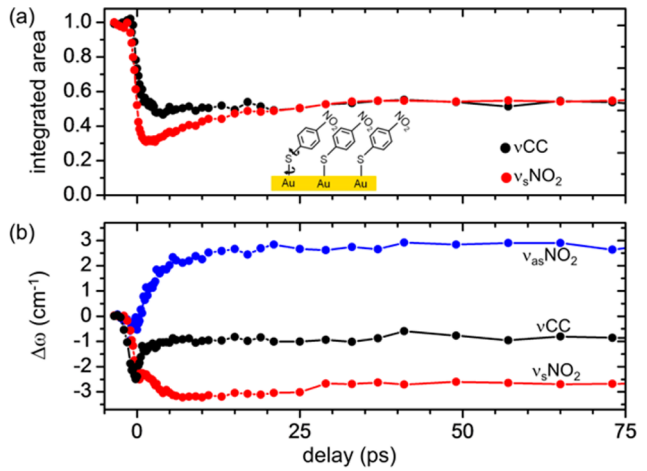

Figure 6. (a) SFG intensity transients for νCC and ν_sNO_2 after flash-heating pulses with ΔT = 190 K. The fractional intensity losses of these two transitions were equal in the longer-time plateau regions. The inset image indicates the conformational coordinates most likely responsible for thermally induced disordering of NBT on Au. (b) Frequency shifts for the three transitions after flash-heating pulses with ΔT = 190 K. The shifts for ν_sNO_2 and $\nu_{as}NO_2$ were equal and opposite in magnitude, and the shifts for both transitions grew in synchronously.

dx.doi.org/10.1021/jp410728j | J. Phys. Chem. B XXXX, XXX, XXX−XXX

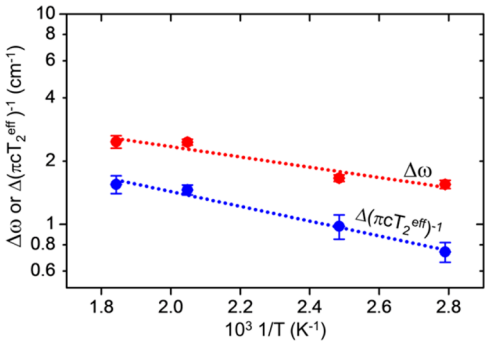

Figure 7. Arrhenius plots of the shifts $\Delta\omega$ and line width increases, plotted as $\Delta(\pi c T_2^{\text{eff}})^{-1}$, for the $\nu_s NO_2$ transition after flash heating.

$M^{(1)}$ of the spectrum, and the width parameter $\Delta(\pi c T_2^{\text{eff}})^{-1}$ was determined from the second moment, using the relation $[M^{(2)}]^{1/2} = \Delta(\pi c T_2^{\text{eff}})^{-1}$. Figure 7 shows that the shift and width Arrhenius plots were roughly but not exactly parallel. The activation energy for the shift was E_a = 390 (±75) cm^{-1}, and for the width, it was E_a = 565 (±75) cm^{-1}. The y-axis intercepts together yielded the values $\Delta\omega$ = 14.6 (±2.9) cm^{-1} and τ = 2.3 (±0.6) ps, and the product is $\Delta\omega\tau$ = 1.0 (±0.25).

4. DISCUSSION

In this section, we will focus on two topics, the origins of the plateau regions in the SFG transients and the application of the vibrational energy exchange model to the $\nu_s NO_2$ data.

The plateau regions represent SAMs in thermal equilibrium with hot Au surfaces. Thermal equilibrium does not preclude the possibility that slower dynamics of the SAM layer have not come into equilibrium during the ~200 ps time interval in which we monitored the SAM after flash heating. In fact, this is clearly not the case because given sufficient time at the higher temperatures, the SAMs would eventually decompose.

In previous works, where we studied flash heating of alkane thiol chains by monitoring the terminal methyl groups, we attributed the SFG intensity loss plateau to orientational disorder of the probed methyl groups resulting from the high temperatures.[2,4] The current study provides additional evidence to support the orientational disorder model for the SFG plateau, based on Figure 6a, which shows that the fractional losses of SFG signals in the plateau regions are identical for both $\nu_s NO_2$ and νCC. The inset in Figure 6a suggests how rotations around Au−S and S−phenyl bonds can cause orientational disorder.

The SFG signal intensity of a transition at frequency ω is proportional to the square of the SFG polarization $P_{\text{SFG}}(\omega)$, which is given by[5]

$$I_{\text{SFG}}(\omega) \propto |P_{\text{SFG}}(\omega)|^2 = |P_R(\omega)|^2 = |[\chi_R^{(2)}(\omega)]E_{IR}E_{vis}|^2 \quad (2)$$

Note that eq 2 lacks the usual nonresonant polarization or susceptibility terms because we are using a nonresonant suppression detection method;[7] therefore, only the resonant R term was observed.

In eq 2, $\chi_R^{(2)}$ is a third-rank tensor. In terms of molecular hyperpolarizability β and number density N

$$\chi_{ijk,R}^{(2)} = N \sum_{abc} \langle (i\cdot a)(j\cdot b)(k\cdot c)\rangle \beta_{abc} \quad (3)$$

where $(i \cdot a)$ is the projection of molecular axis a on lab-frame axis i and $\langle ... \rangle$ is the orientational average.[5] Two key points expressed by eq 3 are that the SFG signal intensity can depend on orientation, for instance, the polar angle θ of the symmetry axis (C_{3v} axis) of an alkanethiol terminal methyl group[24,25] or the C_{2v} axis of the NBT nitro group, and that orientational disorder can reduce the ensemble-averaged orientation, thereby reducing the SFG signals.

In NBT, the $\nu_s NO_2$ and the νCC transitions are both polarized along the nitro C_{2v} axis. For this reason, if the plateau region results from orientational disorder, one would expect the fractional intensity loss for both transitions to be approximately equal, which is what was observed in Figure 6a. The reason that we use the term approximately is that the SFG hyperpolarizability, in the dipole approximation, is proportional to the product of the dipole moment and the Raman polarizability.[26] The dipole moments of $\nu_s NO_2$ and νCC are parallel, but the Raman polarizability tensors are not identical. However, the Raman polarizability tensors for these two transitions are similar and approximately isotropic;[24,25] therefore, for this reason, the orientational dependences of the SFG intensity loss are mostly dependent on the dipole orientation and are thus expected to be approximately the same.

Now, the question is whether the shift and width of the $\nu_s NO_2$ data can be explained by the vibrational energy exchange mechanism. At first glance, the observed differences between the shift and width activation energies disfavor this mechanism. However, now, we will argue that the preponderance of evidence supports the exchange mechanism and that the minor differences in activation energies can be reasonably explained.

In the seminal Harris group studies of durene,[14] the higher-energy probed vibrations were several methyl group CH stretches. Significantly, all of the derived parameters E_a, $\Delta\omega$, and τ were reasonable. The values of E_a were in the 200 cm^{-1} range, which was where methyl group torsions were found, which plausibly have significant anharmonic coupling with the CH stretches. The values of $\Delta\omega$ were 10−20 cm^{-1} and could be positive or negative, the torsion lifetimes were 0.2−0.9 ps, and the values of $\Delta\omega\tau$ were close to +1 or −1.

Using the data in Figure 7, we found the following. Keeping in mind the limited number of data points, there appears to be a single activation energy for the shift and width, but they are not quite equal within experimental error. For the shift, E_a = 390 ± 75 cm^{-1}, and for the width, E_a = 565 ± 75 cm^{-1}. The intercepts yielded values of $\Delta\omega$ = 14.6 (±2.9) cm^{-1} and τ = 2.3 (±0.6) ps, and the product $\Delta\omega\tau$ = 1.0 (±0.25). These derived quantities are, therefore, quite reasonable.

The activation energies indicate that the relevant lower-energy mode is in the 400−600 cm^{-1} range. The lower-energy modes that would be expected to have the greatest anharmonic coupling with the nitro stretch $\nu_s NO_2$ would be the nitro torsion and the nitro bend. We would expect the coupling between nitro stretching modes and phenyl ring modes to be much smaller, and that expectation was confirmed by a recent study of vibrational energy in nitrobenzene.[18] Again, on the basis of nitrobenzene, the torsion should be near 50 cm^{-1}.[27] The temperature dependence in Figure 7 does not support the presence of a strong stretch-to-torsion coupling. However, the nitro bend[27] is near 460 cm^{-1}, which is in the energy range indicated by the slopes in Figure 7 and therefore is the mode most likely coupled to $\nu_s NO_2$.

There is additional support for the energy exchange model in the data in Figure 6b, which shows that the T-jump-induced

dx.doi.org/10.1021/jp410728j | J. Phys. Chem. B XXXX, XXX, XXX−XXX

shifts for $\nu_s NO_2$ and $\nu_{as} NO_2$ (in the plateau region) were equal and opposite in sign. These shifts appear to grow in synchronously with the Au surface temperature rise (i.e., the hot electron decay) seen in the reflectivity transient in Figure 1c. These observations point to a common mechanism for the shifts of the two stretch transitions involving thermal excitation of a lower-energy NBT vibration, and there is precedent for such a mechanism. In triatomic molecules such as NO_2, bending modes have symmetric potentials with positive quartic anharmonic constants, antisymmetric stretching modes also have symmetric potentials but with much smaller quartic anharmonic constants, and symmetric stretching modes have asymmetric Morse-like potentials with negative quartic anharmonic constants.[28] Thus, when the $\nu_s NO_2$ and $\nu_{as} NO_2$ transitions involve quartic anharmonic coupling with the same thermally excited lower-energy mode such as the NO_2 bending mode near 460 cm^{-1}, $\nu_s NO_2$ would be expected to red shift, $\nu_{as} NO_2$ would be expected to blue shift, and the magnitudes of these shifts would be expected to be about equal.[28]

We can propose a reasonable explanation for the disagreement between the two activation energies, besides simply saying that the experimental errors are large. The usual formulation of the vibrational energy exchange model ignores the possibility of inhomogeneous broadening arising from vibrations other than the lower- and higher-energy modes in the model or from structural disorder. If there were a small amount of inhomogeneous broadening in the $\nu_s NO_2$ transition, then at the lower temperatures, where the increase in vibrational line width $\Delta(\pi c T_2^{\text{eff}})^{-1}$ could be smaller than or comparable to the inhomogeneous broadening, we would underestimate the value of $\Delta(\pi c T_2^{\text{eff}})^{-1}$. Such an underestimation would slightly flatten the slope of the temperature-dependent line width measurements in Figure 7. That would not only bring the two activation energies into closer agreement but also bring the slopes closer to the ~460 cm^{-1} value expected if the nitro bend were the dominant lower-energy mode.

5. SUMMARY AND CONCLUSIONS

We have extended previous work on flash-heated SAMs in two directions. Instead of looking at a single vibrational transition of the adsorbate molecules, we have now monitored three different vibrational transitions of the NBT SAM. In addition, we have for the first time measured the temperature dependence for the $\nu_s NO_2$ transition, which was possible because of its large SFG cross section.

By looking at multiple transitions, we made an interesting observation relevant to our interpretation of the SFG intensity loss in the plateau region, where the SAM and Au are in thermal equilibrium. The $\nu_s NO_2$ and νCC transitions are both polarized along the molecular long axis, and as seen in Figure 6a, the fractional SFG intensity losses were identical. This observation offers significant support for the orientational disorder interpretation.

The temperature dependences of the $\nu_s NO_2$ line width and shift were interpreted as supporting the vibrational energy exchange model. Even though the activation energies for width and shift were not quite equal, the values of $\Delta\omega$, τ, and E_a were reasonable, based on the idea that the lower-energy mode exchanging energy with $\nu_s NO_2$ would be the ~460 cm^{-1} nitro bending vibration. This idea had additional support from the observation that the frequency shifts of the symmetric and asymmetric nitro stretching transitions were equal and opposite and that those shifts appeared to grow in synchronously. This would be the expected behavior if both stretching transitions had significant anharmonic coupling to the bending vibration. We suggested that the slightly different values of E_a could be understood if $\nu_s NO_2$ had a small amount of inhomogeneous broadening that masked some of the line width increase at lower values of ΔT.

AUTHOR INFORMATION

Corresponding Author

*E-mail: dlott@illinois.edu.

Notes

The authors declare no competing financial interest.

ACKNOWLEDGMENTS

The research described in this study is based on work supported by the U.S. Air Force Office of Scientific Research under Award Number FA9550-09-1-0163 and the Office of Naval Research under Award N00014-11-1-0418.

REFERENCES

(1) Berg, C. M.; Lagutchev, A.; Dlott, D. D. Probing of Molecular Adsorbates on Au Surfaces with Large-Amplitude Temperature Jumps. *J. Appl. Phys.* **2013**, *113*, 183509.
(2) Wang, Z.; Carter, J. A.; Lagutchev, A.; Koh, Y. K.; Seong, N.-H.; Cahill, D. G.; Dlott, D. D. Ultrafast Flash Thermal Conductance of Molecular Chains. *Science* **2007**, *317*, 787−790.
(3) Carter, J. A.; Wang, Z.; Dlott, D. D. Spatially Resolved Vibrational Energy Transfer in Molecular Monolayers. *J. Phys. Chem. A* **2008**, *112*, 3523−3529.
(4) Wang, Z.; Cahill, D. G.; Carter, J. A.; Koh, Y. K.; Lagutchev, A.; Seong, N.-H.; Dlott, D. D. Ultrafast Dynamics of Heat Flow across Molecules. *Chem. Phys.* **2008**, *350*, 31−44.
(5) Carter, J. A.; Wang, Z.; Dlott, D. D. Ultrafast Nonlinear Coherent Vibrational Sum-Frequency Spectroscopy Methods to Study Thermal Conductance of Molecules at Interfaces. *Acc. Chem. Res.* **2009**, *42*, 1343−1351.
(6) Carter, J. A.; Wang, Z.; Fujiwara, H.; Dlott, D. D. Ultrafast Excitation of Molecular Adsorbates on Flash-Heated Gold Surfaces. *J. Phys. Chem. A* **2009**, *113*, 12105−12114.
(7) Lagutchev, A.; Hambir, S. A.; Dlott, D. D. Nonresonant Background Suppression in Broadband Vibrational Sum-Frequency Generation Spectroscopy. *J. Phys. Chem. C* **2007**, *111*, 13645−13647.
(8) Gadzuk, J. W.; Luntz, A. C. On Vibrational Lineshapes of Adsorbed Molecules. *Surf. Sci.* **1984**, *144*, 429−450.
(9) Ueba, H. Vibrational Lineshapes of Adsorbates on Solid Surfaces. *Prog. Surf. Sci.* **1986**, *22*, 181−321.
(10) Segal, D.; Nitzan, A.; Hänggi, P. Thermal Conductance through Molecular Wires. *J. Chem. Phys.* **2003**, *119*, 6840−6855.
(11) Schoenlein, R. W.; Lin, W. Z.; Fujimoto, J. G.; Eesley, G. L. Femtosecond Studies of Nonequilibrium Electronic Processes in Metals. *Phys. Rev. Lett.* **1987**, *58*, 1680−1683.
(12) Manikandan, P.; Carter, J. A.; Dlott, D. D.; Hase, W. L. Effect of Carbon Chain Length on the Dynamics of Heat Transfer at a Gold/Hydrocarbon Interface: Comparison of Simulation with Experiment. *J. Phys. Chem. C* **2011**, *115*, 9622−9628.
(13) Harris, C. B.; Shelby, R. M.; Cornelius, P. A. Effects of Energy Exchange on Vibrational Dephasing Times in Raman Scattering. *Phys. Rev. Lett.* **1977**, *38*, 1415−1419.
(14) Harris, C. B.; Shelby, R. M.; Cornelius, P. A. Intermolecular Energy Exchange as a Mechanism for Vibrational Dephasing in Polyatomic Molecules. *Chem. Phys. Lett.* **1978**, *57*, 8−14.
(15) Shelby, R. M.; Harris, C. B.; Cornelius, P. A. The Origin of Vibrational Dephasing of Polyatomic Molecules in Condensed Phases. *J. Chem. Phys.* **1979**, *70*, 34−41.

(16) Schosser, C. L.; Dlott, D. D. A Picosecond CARS Study of Vibron Dynamics in Molecular Crystals: Temperature Dependence of Homogeneous and Inhomogeneous Linewidths. *J. Chem. Phys.* **1984**, *80*, 1394−1406.
(17) Hess, L. A.; Prasad, P. N. Vibrational Dephasing in Organic Solids: Temperature Dependence of a Raman Active Localized Internal Mode of Naphthalene. *J. Chem. Phys.* **1980**, *72*, 573−579.
(18) Pein, B. C.; Sun, Y.; Dlott, D. D. Unidirectional Vibrational Energy Flow in Nitrobenzene. *J. Phys. Chem. A* **2013**, *117*, 6066−6072.
(19) El'kin, P.; Pulin, V.; Kosterina, E. Structural Dynamic Models and Vibrational Spectra of Nitrobenzene and Nitropyridines. *J. Appl. Spectrosc.* **2005**, *72*, 483−487.
(20) Fu, Y.; Friedman, E. A.; Brown, K. E.; Dlott, D. D. Vibrational Spectroscopy of Nitroaromatic Self-Assembled Monolayers under Extreme Conditions. *Chem. Phys. Lett.* **2011**, *501*, 369−374.
(21) Lagutchev, A.; Lozano, A.; Mukherjee, P.; Hambir, S. A.; Dlott, D. Compact Broadband Vibrational Sum-Frequency Generation Spectrometer with Nonresonant Suppression. *Spectrochim. Acta, Part A* **2010**, *75*, 1289−1296.
(22) Beran, A. The Reflectance Behaviour of Gold at Temperatures up to 500°C. *Mineral. Petrol.* **1985**, *34*, 211−215.
(23) Lagutchev, A. S.; Patterson, J. E.; Huang, W.; Dlott, D. D. Ultrafast Dynamics of Self-Assembled Monolayers under Shock Compression: Effects of Molecular and Substrate Structure. *J. Phys. Chem. B* **2005**, *109*, 5033−5044.
(24) Hirose, C.; Akamatsu, N.; Domen, K. Formulas for the Analysis of Surface Sum-Frequency Generation Spectrum by CH Stretching Modes of Methyl and Methylene Groups. *J. Chem. Phys.* **1992**, *96*, 997−1004.
(25) Hirose, C.; Akamatsu, N.; Domen, K. Formulas for the Analysis of the Surface SFG Spectrum and Transformation Coefficients of Cartesian SFG Tensor Components. *Appl. Spectrosc.* **1992**, *46*, 1051−1072.
(26) Shen, Y. R. *The Principles of Nonlinear Optics*; Wiley: New York, 1984.
(27) Carreira, L. A.; Towns, T. G. Raman Spectra and Barriers to Internal Rotation: Biphenyl and Nitrobenzene. *J. Mol. Struct.* **1977**, *41*, 1−9.
(28) Madsen, D.; Pearman, R.; Gruebele, M. Approximate Factorization of Molecular Potential Surfaces. I. Basic Approach. *J. Chem. Phys.* **1997**, *106*, 5874−5893.